RZ 3901 (#ZUR1505-056) 05/26/2015
Physical Sciences 9 pages

Research Report

Toggling the local electric field with an embedded adatom switch

W. Steurer,[1] B. Schuler,[1] N. Pavliček,[1] L. Gross,[1] I. Scivetti,[2] M. Persson,[2] and G. Meyer[1]

[1]IBM Research – Zurich, 8803 Rüschlikon, Switzerland

[2]Surface Science Research Centre and Department of Chemistry, University of Liverpool, Liverpool L69 3BX, United Kingdom

Toggling the local electric field with an embedded adatom switch

W. Steurer,[†] B. Schuler,[†] N. Pavliček,[†] L. Gross,[†] I. Scivetti,[‡] M. Persson,[‡] and G. Meyer[*,†]

IBM Research-Zurich, 8803 Rüschlikon, Switzerland, and Surface Science Research Centre and Department of Chemistry, University of Liverpool, Liverpool L69 3BX, United Kingdom

E-mail: gme@zurich.ibm.com

Abstract

By means of scanning probe microscopy we demonstrate that Au^+ on NaCl films adsorbs in an embedded, slightly off-centered Cl–Cl bridge position and can be switched between two equivalent mirror-symmetric configurations using the attractive force exerted by a scanning probe tip. Density functional theory calculations demonstrate that the displacement of the Au atom from the centered position of the bridge bond is accompanied by a large lifting of the closest Cl atom leading to significant changes in the local electrostatic field. Our findings suggest that Au^+ can be used to toggle the local electrostatic field.

Keywords

Atomic Switch, Atomic Manipulation, Scanning Probe Microscopy, Density Functional Theory, Insulating Films, Au adatom

Since the first atomic switch demonstrated by Eigler,[1] atomic and molecular switches have been identified for a plethora of adsorbate–substrate systems.[2–18] Interest in these switches arises primarily from their potential applications in molecular electronics as data storage and processing. However, one could also envision using atomic switches to control bond formation, e.g., between a molecule and a metal atom.[19] A possible route to achieve such functionality may be found in switches that are capable of changing the local electric potential, which has been shown to play a decisive role in the chemistry of a molecule.[17,20] Here, we present a single atom switch that could enable such applications by changing the electric field locally. The switch is formed by a single Au^+ that adsorbs in two equivalent off-centered bridge configurations on multilayer NaCl films. The Au^+ forms a linear complex with its two nearest Cl anions, essentially embedding the Au atom into the NaCl film. This complex is strongly tilted and leads to a the formation of an anisotropic electrostatic field. The tilt and thereby the electrostatic field can be reversibly (and repeatedly) toggled by the scanning probe tip.

The Au^+ switch was realized on 2–11 monolayers (ML) thick NaCl films, supported by either Cu(111) or Cu(100) single crystal substrates. The adsorption properties of Au^+, as well as the switching mechanism, were found not to depend on the film thickness and the orientation of the Cu substrate. Therefore, we will primarily present and discuss the re-

[*]To whom correspondence should be addressed

[†]IBM Research-Zurich, 8803 Rüschlikon, Switzerland

[‡]Surface Science Research Centre and Department of Chemistry, University of Liverpool, Liverpool L69 3BX, United Kingdom

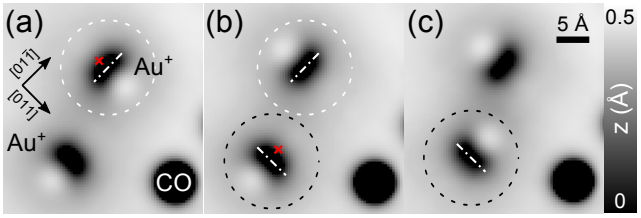

Figure 1: Topographical STM images of stepwise switching of two Au^+ on a NaCl(2ML)/Cu(111) (a–c). The red crosses indicate the lateral tip position in the switching process. The dash-dotted lines indicate the switching axes. The circles serve as a guide to the eye. The arrows in (a) indicate the NaCl lattice directions. Imaging details: constant current feedback ($I = 2\,\mathrm{pA}$, $V = 0.2\,\mathrm{V}$), Xe tip.

sults obtained on NaCl bilayer on Cu(111) [NaCl(2ML)/Cu(111)]. The experiments were performed in a low-temperature scanning tunneling microscope (STM)/atomic force microscope (AFM) based on a qPlus tuning fork sensor design[21] at 5 K. The (bias) voltage was applied to the sample. NaCl films were deposited from a molecular beam evaporator onto a Cu(111) substrate at 270 K. The single crystal substrate was cleaned by repeated cycles of Ne^+ sputtering and short annealing periods at 900 K prior to film preparation. Au atoms were deposited by vacuum sublimation onto the sample at 10 K, leading to neutral adatoms. All data presented here has been acquired with Xe-terminated tips (Xe tips) to enhance the resolution in STM and AFM, although this was not crucial to trigger the Au^+ switch. Therefore, co-adsorbed Xe atoms have been picked up with a clean metal tip.[22]

Au^+ atoms could be formed one at a time on NaCl(2ML)/Cu(111) from neutral Au adatoms by detaching an electron (typically, at $V = -2.5$ V).[23] On a NaCl bilayer this voltage had to be reduced after Au^+ formation as quickly as possible to suppress other current-induced processes, such as NaCl film damage or segregation of Au^+ into the NaCl film.[24] This issue was less problematic on 3 and 4 ML thick films and was absent on thicker films ($\geq$5 ML).

As shown in Figure 1, the STM images of the two formed Au^+ atoms have an asymmetric appearance comprising a protrusion (bright contrast) next to a depression (dark contrast).[23] As we will see later, these two Au^+ atoms adopt equivalent bridge sites that are rotated by 90° with respect to each other. Here, 'bridge site' refers to the Cl–Cl bridge site, which is also a Na–Na bridge site or a hollow site, but not a Na–Cl bridge site. After image acquisition of Figure 1a, the tip was moved to the lateral position indicated by the red cross and the tip–sample distance was decreased until a sudden jump in the frequency shift Δf was observed. The subsequently recorded image (Figure 1b), showed that the respective Au^+ appeared mirror-reflected about a switching axis (indicated by the dash-dotted line). Note, the other Au^+ was switched in a similar manner, as depicted in Figure 1b,c. Note that the voltage was zero during the switching event.

The observation of a strong dependence on the tip position of the switching events during AFM imaging in the constant-height mode sheds more light on the mechanism behind the Au^+ switch, as shown in Figure 2. Au^+ appeared as an oval depression surrounding an off-centered protrusion in the Δf channel. Atomic resolution was obtained on the NaCl lattice with bright and dark contrast on the Na and Cl sites, respectively.[25] From this we can assign the adsorption site of Au^+ to be on a line connecting two neighboring Cl sites. Furthermore, the switching occurred about the bridge site. When the fast scan direction was oriented perpendicular to the switching axis (Figure 2a,b), repeated bidirectional switching between the left ('L') and right ('R') states was observed for Au^+ within the center part of one image. In contrast, only a single switching event during one image was observed when the fast scan axis was aligned parallel to the switching axis (Figure 2c,d).

The influence of the tip–sample distance on the switching was analyzed by carrying out Δf line scans in forward and backward directions for different height offsets above the NaCl film. The locations of the line scans are indicated by red and blue arrows in Figure 2a,b.

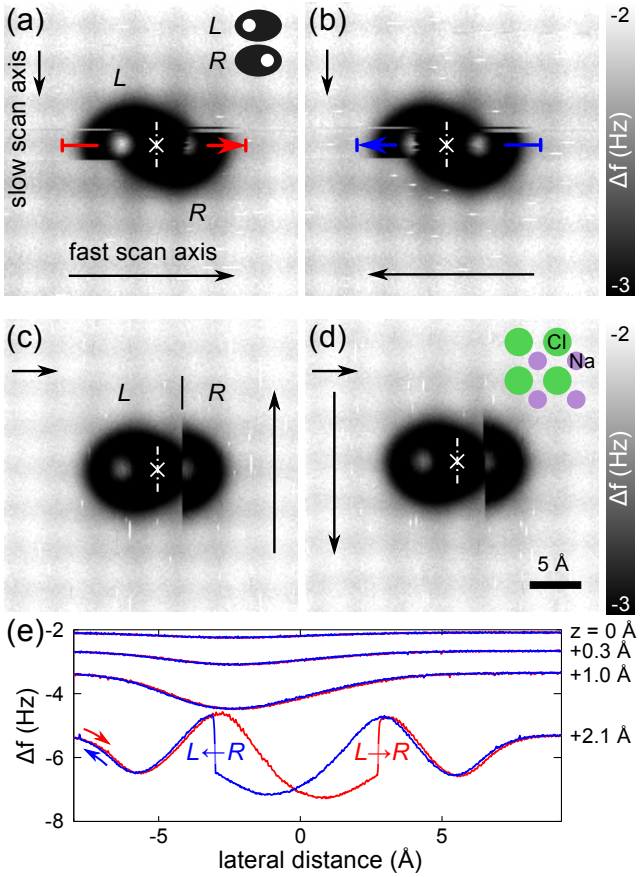

Figure 2: Switching triggered during AFM image acquisition. Fast scan directions (big black arrows) perpendicular (a,b) and parallel (c,d) to the switching axis (dash-dotted line). Slow scan direction is indicated by small black arrows. The bridge site is marked by white crosses in all images. Imaging details: Δf map recorded at constant height, sample bias $V = 0$ V, height offset $z = 2.1$ Å. (e) Δf line profiles recorded at different z values at the position indicated by the red and blue arrows in (a). Data recorded with a Xe tip.

Only a selection of the data is shown in Figure 2e for the sake of clarity. Au^+ was initially in the 'L' state. The top three curves, which were recorded at the largest tip–sample distances, show a featureless depression at a lateral distance of -3 Å with respect to the symmetry axis. At a height set point comparable to the one in Figure 2a–d, $z = 2.1$ Å, a hillock appears in the center of the depression. Tip heights are given with respect to a tunneling set point of ($I = 2$ pA, $V = 0.2$ V) above NaCl. Furthermore, reversible switching between 'L' and 'R' states was observed in the forward and backward traces. Note that the switching from 'L' to 'R' states occurred almost precisely where the protrusion of the 'R' state was located, and vice versa. The same lateral switching positions were observed for all tip–sample distances between $z = 1.6$ Å and 2.1 Å (not shown here). The Sader–Jarvis formalism,[26] was used to extract the attractive vertical force,[27] $F_z = -200 \pm 40$ pN that was required to actuate the Au^+ switch with this particular tip that was Xe terminated.

The Au^+ switch was also investigated by measuring the local contact potential difference (LCPD) between the tip and the sample by Kelvin probe force microscopy (KPFM).[28] A map of the measured LCPD of the 'R' state is shown in Figure 3a. One can recognize an LCPD decrease on the left (blueish contrast) and an LCPD increase on the right (reddish contrast), indicative of a positive and negative local charge, respectively. Line scans of LCPD and Δf at compensated LCPD (Δf^*) across the Au^+ switching axis at different heights are plotted in Figure 3b and 3c, respectively. For the 'R' state, the LCPD is increased to the right, where Δf^* is most attractive. This attractive force is explained by the electrostatic interaction between the negative local charge of the sample and the positively charged Xe tip.[25] After switching from the 'R'- to 'L'-state (Figure 3e,f), the LCPD contrast is essentially reversed and the attractive part is now to the left. Furthermore, the features with most positive LCPD in Figure 3 emerge at the position of the bright protrusion of the respective state shown in Figure 2. Note that the LCPD contrast above the positive charge decays faster than the one above the negative charge with increasing tip height, which we ascribe to a topographic effect as discussed below.

The atomistic nature of the Au^+ switch was revealed from density functional theory (DFT) calculations using a recently developed method that is able to handle different charged adsorbate states on insulating films supported by a metal substrate in a controlled manner.[29,30] This method has been implemented in the `VASP` code[31,32] and is based on a perfect conductor

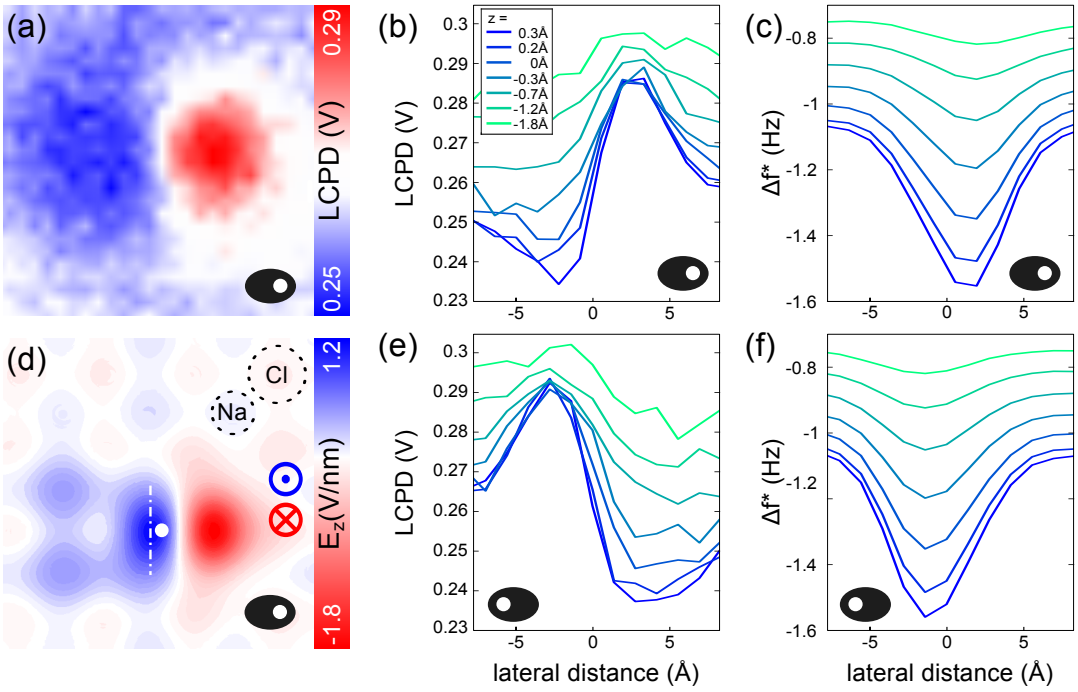

Figure 3: (a) Local contact potential difference (LCPD) map (z = 0 Å, image size: 15×15 Å^2). (b,c) LCPD and corresponding Δf at compensated LCPD (Δf^*) line scans at different heights. (d) Calculated electric field at a distance of 5 Å above the top NaCl layer by DFT. The switching axis is indicated by a dash-dotted line. The position of the Au atom is indicated by the dot. In (a–d) Au^+ is in the 'R' state. (e,f) LCPD and Δf^* line scans at different heights, with Au^+ in the 'L' state. The measurements were recorded with a Xe tip.

(PC) model to approximate the electrostatic response of the metal substrate, while the film and the adsorbate are both treated fully within DFT. The remaining interactions between the metal substrate and the film in the PC approximation were modeled by a simple force field with parameters obtained from DFT calculations of the film and the substrate. The commensurate p(3×3) NaCl bilayer on Cu(100) was represented by a slab geometry in a supercell, where each NaCl layer is composed of 16 Na and 16 Cl atoms. The vacuum region was 23 Å. The plane wave cutoff energy was 400 eV. The surface Brillouin zone was sampled with 2×2 k-points and the structural relaxations were carried out until the forces were less than 0.02 eV/Å. The exchange-correlation effects were treated using the optB86b version of the van der Waals (vdW) density functional.[33–36] The Au^+ state was obtained by constraining the Au adatom and the NaCl bilayer to be positively charged. One meta-stable centered bridge configuration and two equivalent off-centered configurations for Au^+ were identified in the calculations, as schematically shown in Figure 4. The latter configurations were found to be slightly more stable than the former configuration by 40 meV. Another possibility would be adsorption on top of a Na atom, but this configuration was found to be less stable than the off-centered configuration by 300 meV.

As shown in Figure 4, Au^+ forms essentially a linear complex, $(AuCl_2)^-$, with two Cl anions in both the centered and off-centered configuration. In the centered configuration, the linear complex is parallel to the surface, whereas in the off-centered configuration, it is tilted by about 10°. This complex is very similar to the $AuCl_2$ quasi-molecule on a chlorinated Au(111) surface as identified by DFT calculations and STM imaging.[37] Furthermore, the Au^+ complex resembles the Ag^+ complex on NaCl(2ML)/Cu(111)[38] but in the latter case the complex is bent and only a centered configuration was identified. The formation of the tilted $(AuCl_2)^-$ complex gives rise to large

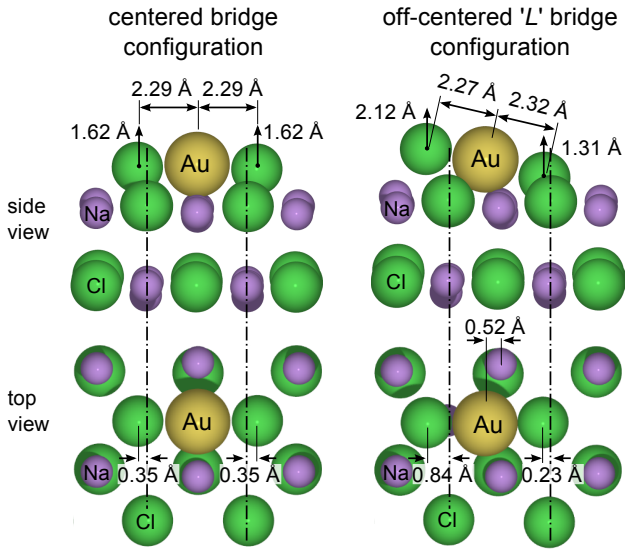

Figure 4: Geometric structure of the Au^+ switch, as obtained from DFT calculations, showing the metastable centered bridge configuration and the 'L'-state of the two equivalent off-centered bridge configurations. Some key interatomic distances and displacements are also indicated.

charge rearrangements as illustrated by the associated large electric field in a plane 5 Å above the top NaCl layer, shown in Figure 3d.

Based on our experimental results and DFT calculations, we relate the protruding features of the Au^+ complex in the STM images shown in Figure 1 and the corresponding protrusions in the AFM images in Figure 2 to the strongly lifted Cl anions of the off-centered and tilted complex. The negative local charge at the position of the bright protrusions in Figure 2a–d, as revealed by the LCPD and Δf^* measurements in Figure 3, supports this assignment. The presence of negative charge on this protruding Cl anion results in the negative electric field in this region shown in Figure 3d. The measured distance of ~ 6 Å between the protrusions of the 'L' and the 'R' states in Figure 2a,b is in agreement with the corresponding calculated distance of 5.8 Å. Finally, note that the two orthogonal orientations of the Au^+ switch, (see Figure 1), are imposed by the bridge adsorption site and the four-fold axial symmetry of the NaCl film.

In addition to the two off-center configurations of Au^+, Au^+ with a symmetric appearance were also observed and are attributed to the center configuration predicted by theory. In particular, this configuration was observed on thicker NaCl films (> 5 ML) and usually right after Au^+ formation. An example of a symmetric Au^+ on NaCl(10ML)/Cu(111) is shown in Ref. 23. In agreement with theory, the symmetric configuration was observed to be metastable. Once the off-center configuration had been triggered by the tip, the centered configuration could only be restored by intermediately neutralizing the Au adatom. Note that the orientation of the Au^+ switch could be changed in a non-deterministic manner between the two orthogonal orientations, using the charge manipulation sequence: $Au^+ \rightarrow Au^0 \rightarrow Au^+$ in which the Au^0 adatom resides in an on-top Cl site.[23]

The atomistic insight into the nature of the Au^+ complex gained from our experiments and DFT calculations suggests a force-actuated switching mechanism. According to Figure 2, the switching occurred always at the position of the lower-lying Cl anion in the tilted, linear $(AuCl_2)^-$ complex. The attractive force exerted by the tip 'pulled' this Cl anion atom upwards and forced the other Cl atom to move down, in analogy to a rocker switch. As a consequence, two bright protrusions shown in Figure 2a,b, which are mirrored about the switching axis, correspond to the lifted Cl atoms in both conformations of the switch. Switching induced by tunneling electrons can be excluded since the switching occurred at zero voltage applied. The Au^+ switch is thus an example of a purely force-actuated atom switch.

Actuation of the Au^+ switch causes the LCPD to change locally by several tens of meV according to Figure 3a. Note that the magnitude of this change is tip and height dependent. The DFT calculations (Figure 3d) show that this actuation results in a change of the local electric field by a few 100 meV/nm at a height of 5 Å in the vicinity of the complex. Recent work has shown that properties of single molecules and molecular ensembles can be influenced by changing their local chemical environment.[12,17,20,39] For example, the orbital se-

quence of single Cu-phthalocyanine molecules could be controlled by changing the distance between Au and Ag atoms placed in the proximity of the molecule.[17] In a similar fashion, the intramolecular hydrogen-transfer reactions in single porphycene molecules on a Cu(110) surface could be controlled by placing a Cu atom nearby.[20] These examples indicate that the Au^+ switch could be used to control the properties of single molecules through its electrostatic field. Importantly, the $(AuCl_2)^-$ complex that is formed is embedded in the NaCl film, which makes this switch especially robust against external perturbations.

In conclusion, we have presented a two-state embedded adatom switch realized with a single Au^+ adsorbed on multilayer NaCl films supported by Cu substrates. The two states are formed by energetically equivalent off-center positions of Au^+ at the bridge site, which can repeatedly, directed and reversibly be switched by the attractive force exerted by the tip of a scanning probe microscope. Measurements of the LCPD show that switching between these two states changes the local electrostatic field and thus the chemical environment. Finally, the purely force-induced actuation of the switch ensures its application also on thick insulating NaCl films.

Acknowledgement We thank R. Allenspach for helpful comments. Financial support by the EU project 'ARTIST' (Contract No. 243421), 'QTea' (317485), 'PAMS' (610446), the ERC Advanced Grant 'CEMAS' (291194), 'The Leverhulme Trust' (F/00 025/AQ), and the allocations of computer resources at ARCHER through MCC (EPSRC (EP/L000202)) and at the PDC Centre for High Performance Computing through SNIC are acknowledged.

Notes The authors declare no competing financial interest.

References

(1) Eigler, D. M.; Lutz, C. P.; Rudge, W. E. *Nature* **1991**, *352*, 600–603.

(2) Quaade, U.; Stokbro, K.; Thirstrup, C.; Grey, F. *Surf. Sci.* **1998**, *415*, L1037–L1045.

(3) Donhauser, Z. J.; Mantooth, B. A.; Kelly, K. F.; Bumm, L. A.; Monnell, J. D.; Stapleton, J. J.; Price, D. W.; Rawlett, A. M.; Allara, D. L.; Tour, J. M.; Weiss, P. S. *Science* **2001**, *292*, 2303–2307.

(4) Moresco, F.; Meyer, G.; Rieder, K.-H.; Tang, H.; Gourdon, A.; Joachim, C. *Phys. Rev. Lett.* **2001**, *86*, 672–675.

(5) Loppacher, C.; Guggisberg, M.; Pfeiffer, O.; Meyer, E.; Bammerlin, M.; Lüthi, R.; Schlittler, R.; Gimzewski, J. K.; Tang, H.; Joachim, C. *Phys. Rev. Lett.* **2003**, *90*, 066107.

(6) Repp, J.; Meyer, G.; Olsson, F. E.; Persson, M. *Science* **2004**, *305*, 493–495.

(7) Alemani, M.; Peters, M. V.; Hecht, S.; Rieder, K.-H.; Moresco, F.; Grill, L. *J. Am. Chem. Soc.* **2006**, *128*, 14446–14447.

(8) Grill, L.; Rieder, K.-H.; Moresco, F.; Stojkovic, S.; Gourdon, A.; Joachim, C. *Nano Lett.* **2006**, *6*, 2685–2689.

(9) Liljeroth, P.; Repp, J.; Meyer, G. *Science* **2007**, *317*, 1203–1206.

(10) Teichmann, K.; Wenderoth, M.; Loth, S.; Ulbrich, R. G.; Garleff, J. K.; Wijnheijmer, A. P.; Koenraad, P. M. *Phys. Rev. Lett.* **2008**, *101*, 076103.

(11) Hasegawa, T.; Ohno, T.; Terabe, K.; Tsuruoka, T.; Nakayama, T.; Gimzewski, J. K.; Aono, M. *Adv. Mater.* **2010**, *22*, 1831–1834.

(12) Wang, Y.; Ge, X.; Schull, G.; Berndt, R.; Tang, H.; Bornholdt, C.; Koehler, F.; Herges, R. *J. Am. Chem. Soc.* **2010**, *132*, 1196–1197.

(13) Mohn, F.; Repp, J.; Gross, L.; Meyer, G.; Dyer, M. S.; Persson, M. *Phys. Rev. Lett.* **2010**, *105*, 266102.

(14) Sweetman, A.; Jarvis, S.; Danza, R.; Bamidele, J.; Gangopadhyay, S.; Shaw, G. A.; Kantorovich, L.; Moriarty, P. *Phys. Rev. Lett.* **2011**, *106*, 136101.

(15) Leoni, T.; Guillermet, O.; Walch, H.; Langlais, V.; Scheuermann, A.; Bonvoisin, J.; Gauthier, S. *Phys. Rev. Lett.* **2011**, *106*, 216103.

(16) Loth, S.; Baumann, S.; Lutz, C. P.; Eigler, D. M.; Heinrich, A. J. *Science* **2012**, *335*, 196–199.

(17) Uhlmann, C.; Swart, I.; Repp, J. *Nano Lett.* **2013**, *13*, 777–780.

(18) Berger, J.; Spadafora, E. J.; Mutombo, P.; Jelínek, P.; Švec, M. *Small* **2015**,

(19) Repp, J.; Meyer, G.; Paavilainen, S.; Olsson, F. E.; Persson, M. *Science* **2006**, *312*, 1196–1199.

(20) Kumagai, T.; Hanke, F.; Gawinkowski, S.; Sharp, J.; Kotsis, K.; Waluk, J.; Persson, M.; Grill, L. *Nat. Chem.* **2014**, *6*, 41–46.

(21) Giessibl, F. J. *Appl. Phys. Lett.* **1998**, *73*, 3956–3958.

(22) Mohn, F.; Schuler, B.; Gross, L.; Meyer, G. *Appl. Phys. Lett.* **2013**, *102*, 073109.

(23) Steurer, W.; Repp, J.; Gross, L.; Scivetti, I.; Persson, M.; Meyer, G. *Phys. Rev. Lett.* **2015**, *114*, 036801.

(24) Li, Z.; Chen, H.-Y.; Schouteden, K.; Lauwaet, K.; Giordano, L.; Trioni, M.; Janssens, E.; Iancu, V.; Van Haesendonck, C.; Lievens, P.; Pacchioni, G. *Phys. Rev. Lett.* **2014**, *112*, 026102.

(25) Gross, L.; Schuler, B.; Mohn, F.; Moll, N.; Pavlicek, N.; Steurer, W.; Scivetti, I.; Kotsis, K.; Persson, M.; Meyer, G. *Phys. Rev. B* **2014**, *90*, 155455.

(26) Sader, J. E.; Jarvis, S. P. *Appl. Phys. Lett.* **2004**, *84*, 1801–1803.

(27) Ternes, M.; Lutz, C. P.; Hirjibehedin, C. F.; Giessibl, F. J.; Heinrich, A. J. *Science* **2008**, *319*, 1066–1069.

(28) Sadewasser, S.; Glatzel, T. *Kelvin probe force microscopy: measuring and compensating electrostatic forces*; Springer, 2011; Vol. 48.

(29) Scivetti, I.; Persson, M. *J. Phys.: Condens. Matter* **2013**, *25*, 355006.

(30) Scivetti, I.; Persson, M. *J. Phys.: Condens. Matter* **2014**, *26*, 135003.

(31) Kresse, G.; Furthmüller, J. *Phys. Rev. B* **1996**, *54*, 11169–11186.

(32) Kresse, G.; Joubert, D. *Phys. Rev. B* **1999**, *59*, 1758–1775.

(33) Dion, M.; Rydberg, H.; Schröder, E.; Langreth, D. C.; Lundqvist, B. I. *Phys. Rev. Lett.* **2004**, *92*, 246401.

(34) Thonhauser, T.; Cooper, V. R.; Li, S.; Puzder, A.; Hyldgaard, P.; Langreth, D. C. *Phys Rev. B* **2007**, *76*, 125112.

(35) Román-Pérez, G.; Soler, J. M. *Phys. Rev. Lett.* **2009**, *103*, 096102.

(36) Klimeš, J.; Bowler, D. R.; Michaelides, A. *Phys. Rev. B* **2011**, *83*, 195131.

(37) Andryushechkin, B. V.; Cherkez, V. V.; Gladchenko, E. V.; Pavlova, T. V.; Zhidomirov, G. M.; Kierren, B.; Didiot, C.; Fagot-Revurat, Y.; Malterre, D.; Eltsov, K. N. *J. Phys. Chem. C* **2013**, *117*, 24948–24954.

(38) Olsson, F. E.; Paavilainen, S.; Persson, M.; Repp, J.; Meyer, G. *Phys. Rev. Lett.* **2007**, *98*, 176803.

(39) Piva, P. G.; DiLabio, G. A.; Pitters, J. L.; Zikovsky, J.; Rezeq, M.; Dogel, S.; Hofer, W. A.; Wolkow, R. A. *Nature* **2005**, *435*, 658–661.

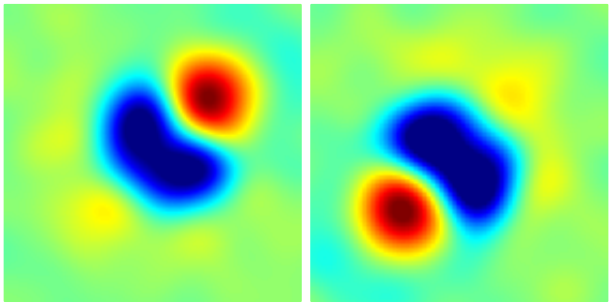

Graphical TOC Entry.